INSTITUTO DE INGENIERÍA ENERGÉTICA
UNIVERSIDAD POLITÉCNICA DE VALENCIA

CPI, Edificio 8E, Cubo F, 5ª planta, Camino de Vera s/n, 46022 Valencia, Spain Tel. (34) 963877270, Fax (34) 963877272, Email: energeti@upvnet.upv.es

INSTITUTO DE INGENIERÍA ENERGÉTICA
(Institute for Energy Engineering)

Research Publications

Available online at www.sciencedirect.com
ScienceDirect
International Journal of Refrigeration 30 (2007) 1004–1017
REVUE INTERNATIONALE DU FROID
INTERNATIONAL JOURNAL OF
refrigeration
www.elsevier.com/locate/ijrefrig

Assessment of boiling heat transfer correlations in the modelling of fin and tube heat exchangers

J.R. García-Cascales[a,*], F. Vera-García[a], J.M. Corberán-Salvador[b], J. Gonzálvez-Maciá[b], David Fuentes-Díaz[b]

[a]*Thermal and Fluid Engineering Department, Universidad Politécnica de Cartagena, 30202 Murcia, Spain*
[b]*Applied Thermodynamics Department, Universidad Politécnica de Valencia, Spain*

Received 4 September 2006; received in revised form 7 November 2006; accepted 9 January 2007
Available online 18 January 2007

Abstract

A new way to assess the performance of refrigeration system models is presented in this paper, based on the estimation of cycle parameters, such as the evaporation temperature which will determine the validity of the method. This paper is the first of a series which will also study the influence of the heat transfer coefficient models on the estimation of the refrigeration cycle parameters. It focuses on fin and tube evaporators and includes the dehumidification process of humid air. The flow through the heat exchanger is considered to be steady and the refrigerant flow inside the tubes is considered one-dimensional. The evaporator model is discretised in cells where 1D mass, momentum and energy conservation equations are solved by using an iterative procedure called SEWTLE. This procedure is based on decoupling the calculation of the fluid flows from each other assuming that the tube temperature field is known at each fluid iteration. Special attention is paid to the correlations utilised for the evaluation of heat transfer coefficients as well as the friction factor on the air and on the refrigerant side. A comparison between calculated values and measured results is made on the basis of the evaporation temperature. The experimental results used in this work correspond to an air-to-water heat pump and have been obtained by using *R*-22 and *R*-290 as refrigerants.

Keywords: Refrigeration; Air conditioning; Heat exchanger; Finned tube; Survey; Correlation; Boiling; Heat transfer; Comparison; Experiment

Evaluation des corrélations de transfert de chaleur lors de l'ébullition dans la modélisation des échangeurs de chaleur du type tube aileté

Mots clés : Réfrigération ; Conditionnement d'air ; Échangeur de chaleur ; Tube aileté ; Enquête ; Corrélation ; Ébullition ; Transfert de chaleur ; Comparaison ; Expérimentation

* Corresponding author. Tel.: +34 968 325 991; fax: +34 968 325 999.
E-mail address: jr.garcia@upct.es (J.R. García-Cascales).

0140-7007/$35.00
doi:10.1016/j.ijrefrig.2007.01.006

Nomenclature

A	cross section area (m^2)
A_o	total surface area
$A_{p,o}$	outer surface area of tubes
$A_{T_{ji}}$	extended surface area
b_w	slope of i vs. T curve
C_p	specific heat (J/kg K)
C_F	function of the molar weight
CV	$G[(x^2/\rho_g\alpha) + ((1-x)^2/\rho_f(1-\alpha))]$
D	diameter (m)
D_c	fin collar outside diameter ($D_o + 2\delta_f$)
D_h	hydraulic diameter (m)
D_o	tube outside diameter
e	wall thickness (m)
$f()$	set of equations
f	friction factor
f_1, f_2, f_3, f_4	friction factor coefficient in air side correlation
$F()$	general function
F_1, F_2, F_3	friction factor coefficient in air side correlation
F_p	fin pitch
g	gravity (m/s^2)
G	mass velocity ($kg/s\,m^2$)
i	enthalpy (J/kg)
j	Colburn factor
k	thermal conductivity (W/m K)
$\dot{m}$	mass flow rate (kg/s)
N	number of tube rows
Nu	Nusselt number
p	pressure (Pa)
P	perimeter (m)
$P_1, P_2, P_3, P_4, P_5, P_6$	Colburn factor coefficients
P_l	longitudinal pitch
P_t	transverse tube pitch
Pr	Prandtl number
q	heat flux (W/m^2)
Q	heat (W)
R	thermal resistance
Re	Reynolds number
S	slip ratio
T	temperature (K)
u	velocity (m/s)
W	humidity (kg vap/kg dry air)
x	vapour quality
z, y	spatial co-ordinates (m)

Greeks

α	heat transfer coefficient (W/m^2 K)
α_c	convection heat transfer coefficient (W/m^2 K)
α_D	convection mass transfer coefficient (W/m^2 K)
δ	film thickness
δ_f	fin thickness
Δ	Increment
ϵ	void fraction
η	dynamic viscosity (Ns/m^2)
η_T	extended surface efficiency
∇^2	Laplacian operator
Φ_f^2	2-phase fric. multiplier
ϕ, φ	generic variable
ϕ	friction multiplier
ρ	density (kg/m^3)
σ	surface tension
θ	angle characterising the volume occupied by the vapour phase

Subscripts and superscripts

a	air
cb	convective boiling
cri	critical
eq	equivalent
f	saturated liquid (liquid phase)
g	saturated vapour (vapour phase)
GO	vapour only
i	inlet, cell index
j	cell index
LO	liquid only
mom	momentum
nb	nucleate boiling
o	outlet, cell index
PB	pool boiling
r	refrigerant
s	saturation
tp	two-phase flow
VO	vapour only
w, W	wall
wat	water
0	reference value
*	reduced parameter

1. Introduction

In this paper, a new way to assess the goodness of published boiling heat transfer correlations for horizontal tubes in fin and tube evaporators calculations is presented.

Normally when a model for fin and tube evaporators is based on cell discretisation, the uncertainties associated with the heat transfer coefficients in both sides overcome those associated with the modelling assumptions. It is also usual to find that the modeller doubts about the application

of correlations which have been developed in conditions which are different from those found in real equipment. For instance: in a fin and tube evaporator the working fluid can be different from that employed for developing the correlation; the wall boundary conditions (constant temperature or constant heat flux) are likely to be different; fully developed flow is not reached in the whole heat exchanger due to the presence of elbows; and the presence of oil in the working fluid is not taken into account. For these reasons, the assessment of the most used boiling heat transfer correlations is required comparing the results given by a fin and tube evaporator model with measurements taken from a real unit.

Fin and tube evaporator models can be classified according to the discretisation detail used in one zone global models, two zone global models, tube by tube models, and cell by cell models.

One zone global models assume a global heat transfer coefficient for the whole heat exchanger that can be dependent on variables, such as air flow rate and evaporator global heat flux. The calculation of the heat exchanger uses the ϵ-NTU or LMTD solutions found for single-phase heat exchangers [1].

Two zone global models divide the evaporator in one single-phase zone and another two-phase zone, each one with constant properties and assuming mean heat transfer coefficients [2].

Tube by tube models pose the conservation equations for each tube of the heat exchangers. These models take into account the coil circuitry and use local heat transfer coefficients. Two of the most well known models in the HVAC industry, ORNL HPDM [3] and EVAP-COND [4], employ this approach.

Finally, cell-by-cell models divide the heat exchanger in a number of cells where the conservation equations of mass, momentum, and energy are posed for each stream and the resulting system of equations is solved by iteration. These models also use local heat transfer coefficients in the energy equation (e.g. CYRANO model [5]).

The model proposed here is cell-by-cell, and the most important source of uncertainty comes from the correlations employed for air and refrigerant side. Thus, the proper characterisation of both sides is very important in the modelling process. The thermal resistances are practically balanced, i.e. $(\alpha A)_{\text{refrigerant}} \simeq (\alpha A)_{\text{air}}$ and a lack of accuracy in the evaluation of any of the heat transfer coefficients may yield to an incorrect calculation of the evaporation temperature. After the state-of-the-art study carried out in boiling heat transfer for horizontal tubes, the correlations developed by Cooper [6], Gorenflo, VDI [7], and Wojtan et al., [8] are selected. Their application ranges are suited to the conditions normally found in HVAC.

Numerical tests are run so that the performance of the refrigeration cycle can be compared to the experimental cycle by means of evaporation temperatures. These are carried out in a way that also allows for the simultaneous evaluation of the validity of the numerical method and the heat transfer coefficient correlation employed. The experimental results used in this work correspond to an air-to-water heat pump and have been performed using two different refrigerants: *R*-22 and *R*-290 (propane). In the final sections, the experimental results are compared with the calculated ones, so lastly the final conclusions can be drawn.

2. Fin and tube evaporator model

The heat exchanger is divided into a number of cells where the conservation equations for each side are posed and discretised to give a set of algebraic equations which are solved iteratively by using the SEWTLE procedure [9]. The following section shows the discretisation of the equations for the refrigerant and the strategy employed to solve the resulting set of algebraic equations.

2.1. Refrigerant side governing equations

The assumptions made for the refrigerant flowing inside the tubes are:

- One-dimensional steady flow;
- Negligible longitudinal heat conduction;
- Thermal equilibrium between liquid and vapour;
- Separated flow;
- No internal heat generation;
- Negligible kinetic energy contribution in the energy equation.

The governing equations for a single-phase flow are:

$$G = \rho u = \text{constant} \tag{1}$$

$$\frac{\mathrm{d}p}{\mathrm{d}z} = -\frac{\mathrm{d}(\rho u^2)}{\mathrm{d}z} - f\frac{1}{2}\rho\frac{u^2}{D_\mathrm{h}} - \rho g\sin(\theta) \tag{2}$$

$$\dot{m}\frac{\mathrm{d}i}{\mathrm{d}z} = \alpha P_\mathrm{w}(T_\mathrm{w} - T) \tag{3}$$

which are valid for the refrigerant side whenever its state is single-phase.

In the two phase flow region of the heat exchanger, the separated flow model is considered, and the governing equations are:

$$G = \frac{\dot{m}}{A_\mathrm{c}} = \text{constant} \tag{4}$$

$$-\frac{\mathrm{d}p}{\mathrm{d}z} = \frac{fG^2}{2D_\mathrm{h}\rho_\mathrm{f}}\Phi_\mathrm{fo}^2 + G^2\frac{\mathrm{d}\left(\dfrac{x^2}{\rho_\mathrm{g}\epsilon} + \dfrac{(1-x)^2}{\rho_\mathrm{f}(1-\epsilon)}\right)}{\mathrm{d}z} + \big(\alpha\rho_\mathrm{g} + (1-\epsilon)\rho_\mathrm{f}\big)g\sin\theta \tag{5}$$

$$A_\mathrm{c}G\frac{\partial\big[xi_\mathrm{g} + (1-x)i_\mathrm{f}\big]}{\partial z} + A_\mathrm{c}Gg\sin\theta = P_\mathrm{w}\alpha(T_\mathrm{w} - T) \tag{6}$$

The continuity equation states the conservation of the mass flow rate and the mass velocity along a fluid path

and its value is deduced from the inlet conditions, G will be considered as a known constant in what follows.

In a fluid cell, there are two equations (energy and momentum) to be considered, but eight unknown variables: x, ϵ, ρ_f, ρ_g, i_f, i_g, p and T. The number of equations is clearly lower than the number of unknowns, hence some further relationships among these variables must be stated. First, thermodynamic equilibrium is assumed, allowing the following set of state equations to be added to the system:

$$T = T_{\text{sat}}(p), \quad \rho_{\text{g}} = \rho_{\text{g}}(p), \quad i_{\text{g}} = i_{\text{g}}(p), \quad \rho_{\text{f}} = \rho_{\text{f}}(p), \quad i_{\text{f}} = i_{\text{f}}(p) \tag{7}$$

Now only one equation is missing to close the system. Obviously, some equations which state the relationship between the void fraction and the rest of the variables should be added into the balance

$$\epsilon = \frac{1}{1 + S\dfrac{1-x}{x}\dfrac{\rho_{\text{g}}}{\rho_{\text{f}}}} \tag{8}$$

This equation introduces a new variable, the slip ratio, $S=u_{\text{g}}/u_{\text{f}}$, and, therefore there is still one missing equation. The only way to close the problem is to consider some empirical relationships among those variables. A number of such correlations can be found in the existing literature, for instance in Wallis [10]. The commonly used Chisholm correlation [11] is utilised in this model because it is quite simple and provide accurate results [12].

$$S = \left[1 - x\left(1 - \frac{\rho_{\text{f}}}{\rho_{\text{g}}}\right)\right]^{1/2} \tag{9}$$

Now the system is closed, i.e. there are nine equations combined with nine unknowns.

2.2. Air side governing equations

For the air side, the governing equations are those stated for the mass, energy, and momentum conservation. In the case of the differential surface (Fig. 1), the following approximated equations are obtained:

$$-\dot{m}_{\text{a}}\text{d}i = \text{d}Q - \dot{m}_{\text{a}}\text{d}W i_{\text{f,wat}} \tag{10}$$

$$\text{d}Q = \left[\alpha_{\text{c}}(T - T_{\text{wat}}) + \alpha_{\text{D}}(W - W_{\text{s,wat}})\left(i_{\text{g,t}} - i_{\text{f,wat}}\right)\right]P\text{d}z \tag{11}$$

$$-\dot{m}_{\text{a}}\text{d}W = \alpha_{\text{D}}P\text{d}Z(W - W_{\text{s,wat}}) \tag{12}$$

$$\frac{\text{d}p}{\text{d}z} = -\frac{\text{d}(\rho u^2)}{\text{d}z} - f\frac{\rho u^2}{2D_{\text{h}}} \tag{13}$$

The approach used to treat the dehumidification process is that proposed by Kuehn et al. [13]. Fig. 1 displays an air cell in the more general case in which dehumidification of humid air takes place when it is in contact with a cold surface. Then, a water film is formed on this surface. There is a limit boundary layer of air next to the water surface. The hypothesis that the air in contact with the water film is saturated at the temperature of the water surface, T_{wat}, is assumed.

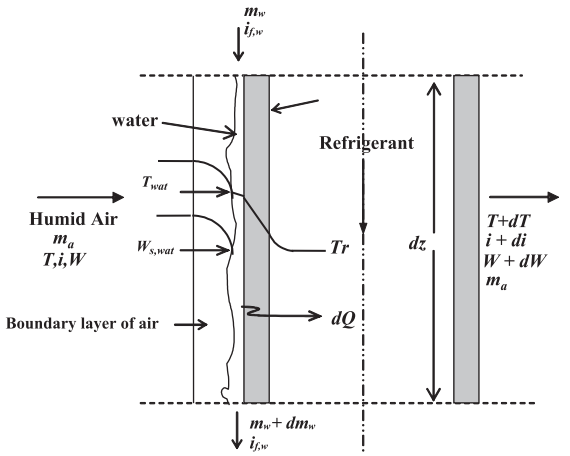

Fig. 1. Cooling and dehumidification of wet air around a tube.

The heat transfer can be expressed as a function of the enthalpy difference and the driving potential in such a way that:

$$\text{d}Q = \frac{\alpha_{\text{w}}}{b_{\text{w}}}(i - i_{\text{s,w}})P\text{d}z \tag{14}$$

where,

$$\alpha_{\text{w}} = \frac{1}{\dfrac{C_{\text{p,a}}}{b_{\text{w}}\alpha_{\text{c}}} + \dfrac{y_{\text{w}}}{k_{\text{w}}}} \tag{15}$$

with k_{w} being the water thermal conductivity, and y_{w} the thickness of the water film.

The value for α_{c} comes from semi-empirical correlations. In the model, those proposed by Chi Chuang Wang et al. [14] are used as default correlations for both sensible heat transfer and dehumidifying conditions.

2.3. Global solution strategy

The global solution method for the calculation of the heat exchanger is called SEWTLE (Semi Explicit method for Wall Temperature Linked Equations) and is described in [9]. In the case of air to refrigerant heat transfer, it can be implemented in the following way.

In single-phase flow, the momentum and energy equations are decoupled (Eqs. (2) and (3)), leading to the possibility of using first the energy equation (Eq. (3)) along with the equations of state to calculate the temperature solution at the outlet of the fluid cell. The momentum equation (Eq. (2)) can then be used to calculate the pressure and density variation.

The discretisation employed for the energy equation is based on a linear fluid temperature variation (LFTV scheme) which leads to:

$$T^{\text{out}} = \frac{(1 - 0.5\Delta x_i \chi)T_i + \Delta x \chi T_w}{1 + 0.5\Delta x \chi} \tag{16}$$

where,

$$\chi = \frac{P_w \alpha}{\dot{m} C_p} \tag{17}$$

in which T^{out} and T^{in} are the cell outlet and inlet temperatures respectively, Δx is the cell length, P_w is the wetted perimeter, h the heat transfer coefficient, $\dot{m}$ the mass flow rate, and C_p the isobaric heat capacity.

In two phase flow, the momentum and energy equations (Eqs. (5) and (6)) are coupled by pressure. Fortunately, as the dependency is weak due to the usual small pressure drop inside the heat exchanger, the momentum equation may be integrated first. Once the pressure at the outlet of the fluid cell is known, the energy equation can be integrated, leading to the evaluation of the enthalpy, the vapour quality, and the rest of variables at the outlet.

A simple, but proved effective, discretisation is adopted for the momentum equation. The friction and gravity terms are approached by the arithmetic average value of the corresponding function multiplied by the increment in distance along the channel. The acceleration term is integrated as the difference between the outlet and the inlet values.

$$p_o = p_i - \left[\overline{\frac{fG^2}{2D_h \rho_f}\phi_{fo}^2}\right]\Delta Z + G[\text{CV}_o - \text{CV}_i]^* + \left(\overline{\epsilon\rho_g + (1-\epsilon)\rho_f}\right) g \sin\theta \Delta Z \tag{18}$$

where * means 'evaluated at previous iteration' and CV stands for

$$\text{CV} = G\left[\frac{x^2}{\rho_g \epsilon} + \frac{(1-x)^2}{\rho_f(1-\epsilon)}\right] \tag{19}$$

The arithmetic averages in Eq. (18) require the knowledge of the outlet conditions. As such, the values employed are updated by using the present value at the inlet plus a variation of ç the property along the cell, by assuming that the variation is the same as that obtained in the previous iteration:

Outlet value: $\phi_o = \phi_i + (\phi_o - \phi_i)^*$
Average value: $\overline{\phi} = \phi_i + ((\phi_o - \phi_i)^*/2)$

Once the outlet pressure is calculated, then both the thermophysical properties of the fluid, and the temperature are calculated. The energy equation can be discretised as in single-phase flow using the LFTV scheme, providing the outlet enthalpy by means of the following expression:

$$i_o = i_i + \frac{\alpha}{\dot{m}}\left(T_w - \frac{T_i + T_o}{2}\right)P_w \Delta z - g \sin\theta \Delta z \tag{20}$$

On the air side, in the case in which there is air dehumidification, the energy equation (Eq. (14)) is integrated, calculating first the outlet enthalpy and then the outlet temperature,

$$i_o = i_i \exp\left(-\frac{\alpha_w P \Delta z}{\dot{m}_a b_w}\right) + h_{s,w}\left(1 - \exp\left(-\frac{\alpha_w P \Delta z}{\dot{m}_a b_w}\right)\right) \tag{21}$$

$$T_o = T_i \exp\left(\frac{-\alpha_c P_w \Delta Z}{\dot{m}_a C_{p,a}}\right) + T_w\left(1 - \exp\left(\frac{-\alpha_c P_w \Delta Z}{\dot{m}_a C_{p,a}}\right)\right) \tag{22}$$

The latent heat is calculated as the difference between the total and the sensible heat. From the latent heat the outlet humidity is obtained. The momentum equation is then integrated, and the outlet pressure of the air is determined. Finally, the outlet properties of the air can be calculated.

Note that the described system of equations is discretised in such a way that the calculation of the outlet conditions at every fluid cells is completely explicit, and also that such a calculation starts from the inlet section of the HE and progresses along every fluid path. However, the iterative nature of the global strategy provides an adequate evaluation of both the thermophysical properties of the fluids and of the friction factor, as well as the heat transfer coefficient at every cell.

Once the refrigerant and air temperature are known at every cell, the wall temperature can be determined by the balance of heat transfer between the fluids and the wall. To determine the wall temperature, T_w, the balance between the heat transferred from the air side to the refrigerant side is stated as:

$$P_{w,a}\Delta Z_a \alpha_{a,eq}(T_{a,i} - T_w) = P_{w,r}\Delta Z_r \alpha_r (T_w - \overline{T}_r) \tag{23}$$

where α_r and $\alpha_{a,eq}$ are defined in such a way that they provide the heat exchanged between the fluids through the equivalent temperature difference. Thus, the equation becomes linear.

The iteration is carried out as follows. First, the air and refrigerant temperatures are calculated. Then, wall temperatures are determined based on fluid temperatures. This procedure is repeated until the heat balance between air and refrigerant has a relative error less than 10^{-6}. The number of required iterations to get the solution usually ranges from 10 to 20.

3. Heat transfer coefficient correlations

In this study, special attention is paid to a few updated correlations which let plain finned horizontal tube heat exchangers be modelled with a high degree of accuracy. In the existing literature, many correlations for characterising boiling inside plain tubes can be found. Some have been

studied by the authors [15], and most of them belong to one of the next three categories:

- Superposition methods (i.e. Chen, [16]).
- Enhancement models (i.e. Shah, [17]).
- Asymptotic models (i.e. Steiner and Taborek [18]).

Superposition and asymptotic models consider two thermal mechanisms, nucleate boiling and convective boiling which are included by means of expressions such as:

$$\alpha_{tp} = \left[\alpha_{nb}^{n} + \alpha_{cb}^{n}\right]^{1/n} \tag{24}$$

where $n = 1$ for Chen correlation [16], $n = 2$ for Kutateladze's [19], and $n = 3$ for Steiner and Taborek's [18]. Asymptotic methods have been proven to be very suitable for the characterisation of flow boiling, since they cover a wide range of refrigerants and take into account most of the regimes inside the pipes. In the case of horizontal tubes, there are many models that are adaptations of vertical correlations to horizontal test data (Shah, Gungor and Winterton, Klimenko, Kandikar or Wattelet). Some of these models use the Froude number Fr_f to predict the onset of stratification. In general, this fails to reproduce patterns such as stratified flows or local conditions with partial dry-out. Nucleate pool boiling correlations are frequently used to account for the nucleate boiling contribution to the heat transfer coefficient. These are based on:

- Physical properties (i.e. Stephan and Abdelsalam [20]).
- Reduced pressure (i.e. Cooper [6]).
- Fluid specific (i.e. Gorenflo correlation, proposed in the VDI Heat Atlas [7]).

With regards to the correlations employed in this work to estimate the heat transfer coefficient, four models have been considered. These include that proposed by Steiner in the VDI Heat Atlas [7] which is an extension of the Steiner–Taborek correlation [18]. The latter was developed for flow boiling inside vertical tubes, and therefore is an asymptotic model. The correlation developed by Wojtan et al. correlation [8] is also used. This considers an asymptotic approach for the non-stratified contribution of the correlation. These two correlations have been compared with nucleate pool boiling correlations, in order to show the influence of this phenomenon in such models. As is mentioned above, one is based on the reduced pressure (Cooper, see [6]) and the other is a fluid specific correlation (Gorenflo correlation) proposed in the VDI Heat Atlas [7].

3.1. Cooper correlation

The correlation proposed by Cooper [6] for the heat transfer coefficient for nucleate pool boiling is a function of the reduced pressure and includes the effect of wall roughness and heat flux. The applicability of this expression in terms of reduced pressure, p_r, and molecular weight, M, is $0.001 \leq p^* \leq 0.9$ and $2 \leq M \leq 200$.

$$\alpha_{pb} = 55 p^{*0.12} \left(\log_{10}(p^*)\right)^{-0.55} M^{-0.5} q^{0.67} \tag{25}$$

3.2. Gorenflo correlation

This correlation, proposed by Gorenflo, is included in the VDI Heat Atlas [7] (Chapter Ha on Pool boiling). It considers a separate treatment of the main groups of variables: properties of the fluids, nature of the heated surfaces, operating parameters, etc.

$$\frac{\alpha}{\alpha_0} = C_W F(p^*) \left(\frac{\dot{q}}{\dot{q}_0}\right)^{n(p^*)}, \tag{26}$$

where C_W stands for the effect of the properties of the heated surface, which may be obtained by the following expression:

$$C_W = \left(\frac{R_a}{R_{a0}}\right)^{0.133}, \tag{27}$$

with $R_{a0} = 0.4$ μm being the roughness parameter reference value.

The effect of the reduced pressure on the correlation is taken into account by means of

$$F(p^*) = 1.2 p^{*0.27} + \left(2.5 + \frac{1}{1 - p^*}\right) p^* \quad \text{for refrigerants.} \tag{28}$$

$(\dot{q}/\dot{q}_0)^{n(p^*)}$ accounts for the effect of heat flux and saturation pressure on the heat transfer coefficient. $n(p^*)$ decreases with a rise in pressure,

$$n = 0.9 - 0.3 p^{*0.3} \quad \text{for halogenated refrigerants.} \tag{29}$$

The reference value α_0 is calculated by using the Stephan and Preusser correlation [22] with a reduced pressure of $p_0^* = 0.1$ and a heat flux of $\dot{q}_0 = 20{,}000\ \mathrm{W/m^2}$. This correlation is given by,

$$\frac{\alpha_1}{\alpha_0} = F_q F_p F_{wr} F_{wm} \tag{30}$$

where,

F_q is a function of the heat flux ratio between the flux at the wall and a reference heat flux;
F_p is a function of the reduced pressure;
F_{wr} takes into account the micro-structure;
F_{wm} considers the material properties.

After substituting their corresponding expressions, the following expression is obtained:

$$\alpha = \frac{k_f}{d_0} \left[\frac{\dot{q}_0 d_0}{\lambda_f T_s}\right]^{0.674} \left[\frac{\rho_g}{\rho_f}\right]^{0.156} \left[\frac{\Delta h_g d_0^2}{a_f^2}\right] \left[\frac{a_f^2 \rho_f}{\sigma d_0}\right]^{0.350} \left[\frac{\eta_f c_{pf}}{\lambda_f}\right] \tag{31}$$

As this equation is only suitable for a reduced pressure of $p_0^* = 0.3$, α_0 is obtained in two steps (see [7] for a complete description). The bubble diameter at departure d_0 is given by,

$$d_0 = 0.0149\beta\left(\frac{2\sigma}{g(\rho_f - \rho_g)}\right)^{0.5} \tag{32}$$

where the contact angle β is 35° for any substance other than water or cryogenic liquids.

The Gorenflo correlation is valid only for values of the reduced pressure $0.1 < p^* < 0.9$, although in [21] it is extended to a wider range $0.05 < p^* < 0.95$.

3.3. VDI Heat Atlas correlation for horizontal tubes

The correlation presented in this section is that proposed by Steiner in the VDI Heat Atlas [7]. The heat transfer coefficient is obtained by means of an asymptotic expression of the form:

$$\alpha = \left(\alpha_{cb}^3 + \alpha_{nb}^3\right)^{1/3}. \tag{33}$$

The convective boiling part of the equation is given by,

$$\frac{\alpha_{cb}}{\alpha_{LO}} = \left\{\left[(1-x) + 1.2x^{0.4}(1-x)^{0.01}\left(\frac{\rho_f}{\rho_g}\right)^{0.37}\right]^{-2.2} + \left[\frac{\alpha_{VO}}{\alpha_{LO}}x^{0.01}\left(1 + 8(1-x)^{0.7}\left(\frac{\rho_f}{\rho_g}\right)^{0.67}\right)^{-2}\right]\right\}^{-0.5}, \tag{34}$$

where α_{LO} and α_{VO} are the local single-phase heat transfer coefficients, and the Reynolds numbers for the liquid and vapour are given by:

$$Re_{LO,VO} = \frac{\dot{m}D_h}{\eta_{L,V}}. \tag{35}$$

The range of validity of this correlation is $3 \le \rho_f/\rho_g \le 1500$ which corresponds to a reduced pressure in the range $5 \times 10^{-3} \le p^* \le 0.8$.

The nucleate boiling contribution to the heat transfer coefficient is given by the expression:

$$\frac{\alpha_{nb}}{\alpha_0} = C_F\left(\frac{\dot{q}}{q_0}\right)^{n(p^*)}F(p^*)F(D)\left(\frac{R_a}{R_{a0}}\right)^{0.133}F(\dot{m},x) \tag{36}$$

where

$$F(\dot{m},x) = \left(\frac{\dot{m}}{\dot{m}_0}\right)^{0.25}\left[1 - p^{*0.1}\left(\frac{\dot{q}}{q_{cri,PB}}\right)^{0.3}x\right], \tag{37}$$

$$F(p^*) = 2.692p^{*0.43} + \frac{1.6p^{*6.5}}{1-p^{*4.4}}. \tag{38}$$

If we have a high thermal conductivity ($\lambda_w s \ge 0.7$ W/K):

$$n(p^*) = 0.8 - 0.13 \times 10^{0.66p^*}, \quad \text{for hydrocarbons and halocarbons,} \tag{39}$$

$$n(p^*) = 0.7 - 0.18 \times 10^{0.38p^*}, \quad \text{for cryogenic fluids.} \tag{40}$$

$$F(D) = \left(\frac{D_0}{D}\right)^{0.5}, \tag{41}$$

where D_0 has a reference value of 10^{-2} m and

$$C_F = 0.73M^{0.11} \tag{42}$$

with a limit value of $C_F \le 2.5$.

The effect of low wall heat conduction due to incomplete wetting is also considered by means of correction parameters which depend on the regime. These parameters affect the heat flux ratio exponent, $n(p^*)$, and the molar mass parameter, C_F [7].

3.4. Wojtan, Ursenbacher and Thome correlation

This model is a modification of that developed by Kattan et al. in Refs. [23–25] and its successive modifications Ref. [26] or Ref. [27]. Unlike other models, turbulent film flow heat transfer is based on the liquid film velocity. Also a wide spectrum of flow patterns is covered, and partial wetting of the tube cross section is taken into account. The heat transfer coefficient correlation for a tube with a diameter D is given by:

$$\alpha_{tp} = \frac{\theta_{dry}\alpha_{vapour} + (2\pi - \theta_{dry})\alpha_{wet}}{2\pi} \tag{43}$$

where α_{wet} represents the heat transfer coefficient on the wet perimeter and is obtained from the asymptotic expression:

$$\alpha_{wet} = \left(\alpha_{nb}^3 + \alpha_{cb}^3\right)^{1/3}. \tag{44}$$

The nucleate boiling contribution is determined by using the Cooper correlation [6] for Eq. (44)

$$\alpha_{nb} = 55p^{*0.12}(-\log_{10}p^*)^{-0.55}M^{-0.5}q^{0.67} \tag{45}$$

and the convective boiling contribution by means of

$$\alpha_{cb} = 0.0133Re_f^{0.69}Pr_f^{0.4}\frac{\lambda_f}{\delta} \tag{46}$$

The Reynolds number, Re_f, is calculated by using the mean liquid velocity in the film:

$$Re_f = \frac{4G(1-x)\delta}{(1-\epsilon)\eta_f}. \tag{47}$$

The void fraction in the previous equations is calculated by using the Rouhani–Axelsson expression:

$$\epsilon = \frac{x}{\rho_g}\left\{[1 + 0.12(1-x)]\left(\frac{x}{\rho_g} + \frac{1-x}{\rho_f}\right) + \frac{1.18}{G}\left[\frac{g\sigma(\rho_f - \rho_g)}{\rho_f^2}\right]^{1/4}(1-x)\right\}^{-1}. \tag{48}$$

The vapour heat transfer coefficient of the dry perimeter, α_{vapour} is evaluated by means of the Dittus–Boelter turbulent flow heat transfer correlation:

$$\alpha_{vapour} = 0.023 Re_g^{0.8} Pr_g^{0.4} \frac{k_g}{D} \quad (49)$$

where the vapour Reynolds number, Re_g, is determined by using the mean vapour mass velocity, G, and the internal tube diameter, D,

$$Re_g = \frac{GxD}{\epsilon \eta_g}. \quad (50)$$

The parameter θ_{dry} stands for the angle occupied by the vapour phase in regimes that involve any kind of stratification, so that it takes the following values depending on the regime,

$\theta_{dry} = 0$ in the case of annular flow.

$\theta_{dry} = \theta_{strat}((G_{wavy} - G)/(G_{wavy} - G_{start}))$ when G lies between G_{strat} and G_{wavy} (values of the mass flux which characterise the change from fully-stratified to stratified-wavy flow, and from stratified-wavy to annular flow, respectively).

$\theta_{dry} = \theta_{strat}$ for fully-stratified flow at mass velocity, G.

The film thickness is given by $\delta = ((\pi D(1-\epsilon))/(2(2\pi - \theta_{dry}))$, and the stratification angle by:

$$\theta_{strat} = 2\pi - 2\left\{\pi(1-\epsilon) + \left(\frac{3\pi}{2}\right)^{1/3}\left[1 - 2(1-\epsilon) + (1-\epsilon)^{1/3} - \epsilon^{1/3}\right] - \frac{1}{200}(1-\epsilon)\epsilon[1-2(1-\epsilon)] \times \left[1 + 4\left((1-\epsilon)^2 + \epsilon^2\right)\right]\right\}, \quad (51)$$

The model is completed with the definition of a map which permits the identification of the pattern developed locally inside the tube. To predict local heat transfer coefficients, the following models are considered in the map: stratified flow; slug + stratified-wavy flow; slug flow; intermittent flow; annular flow; annular flow with dry-out and mist flow [28].

To illustrate the behaviour of these correlations, they are compared in Figs. 2 and 3. The values gathered in these figures correspond to the heat transfer coefficient as a function of the vapour quality for several mass flow rates – 50, 125 and 200 kg/m^2 s – at a fixed heat flux of 4500 W/m^2 and for several heat fluxes – 3000, 6000 and 9000 W/m^2 – at a constant mass flow rate 125 kg/m^2 s. They cover the range of practical cases analysed in the experiments where the mass flow rate ranges from 50 to 75 kg/m^2 s in the case of R-290 and from 100 to 200 kg/m^2 s in the case of R-22 (Fig. 2), and where the heat flux has varied roughly between 3000 and 6000 W/m^2 in the case of R-290 and between 3000 and 9000 W/m^2 in the case of R-22 (Fig. 3). The evaporation pressure considered in the calculations is $p = 5$ bar, with a horizontal tube diameter $D_h = 11.9 \times 10^{-3}$ m and R-22 as the refrigerant. Important differences are found between the Wotjan et al. correlation and the others when the mass flow rate increases and the nucleate boiling contribution in this correlation becomes less important as annular flow is

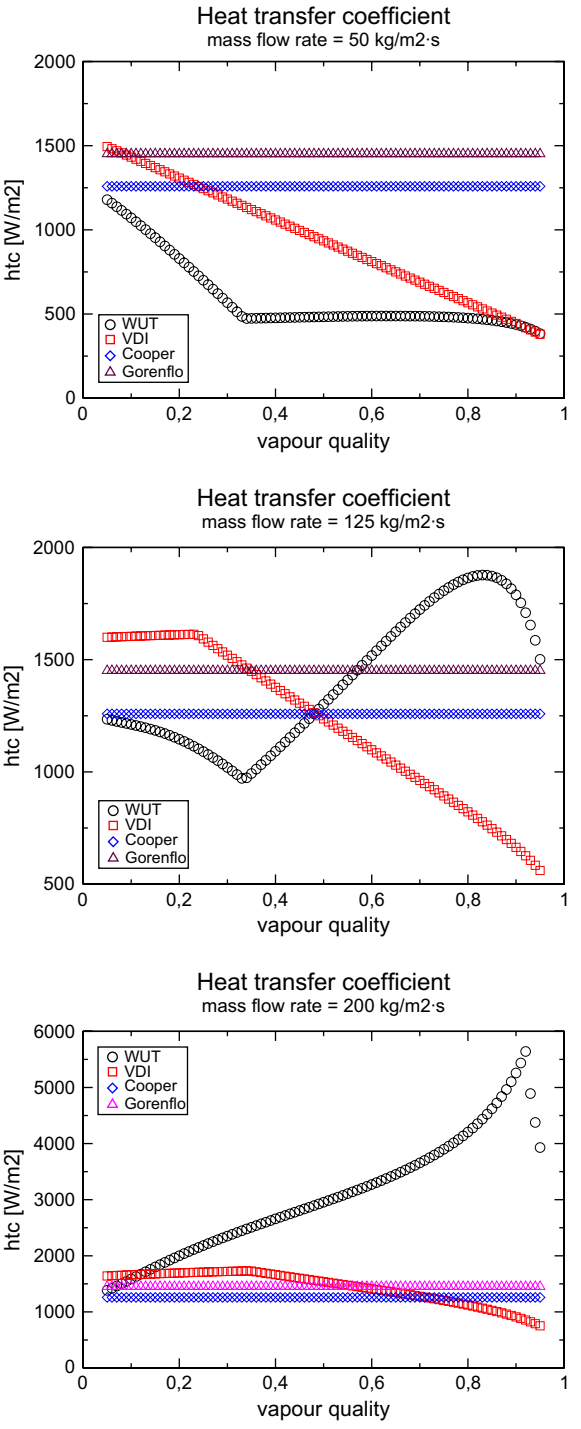

Fig. 2. Heat transfer coefficient at different mass flow rates (50, 125 and 200 kg/m^2 s) and constant heat flux $q = 4{,}500$ W/m^2.

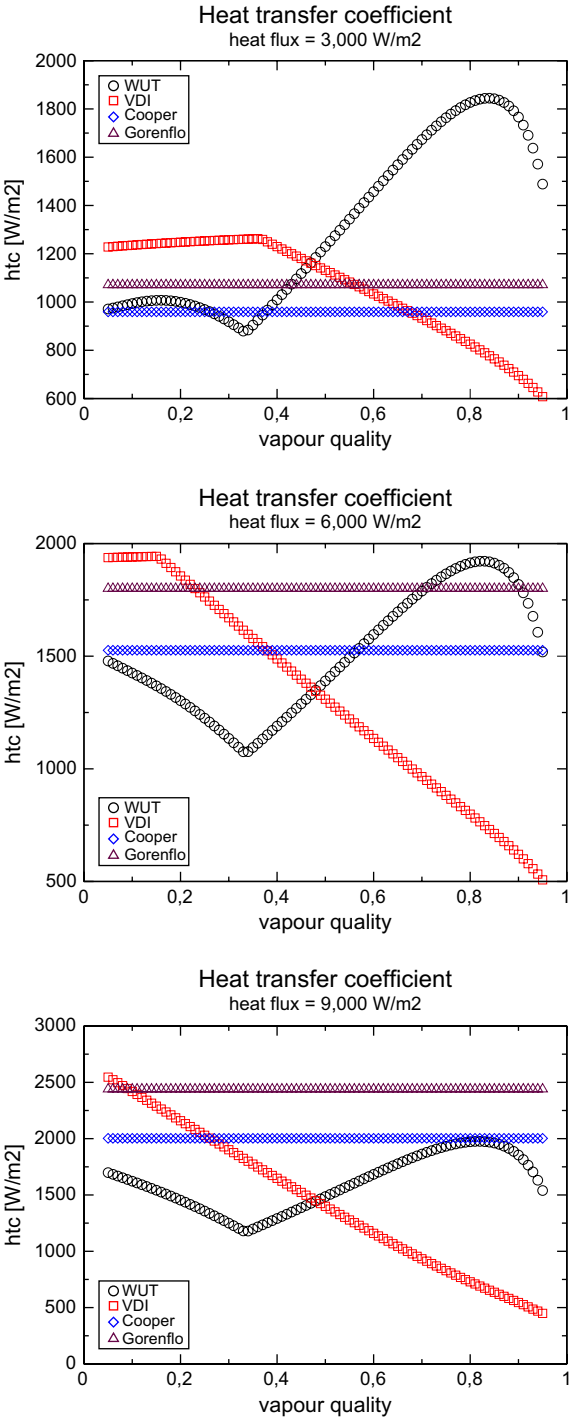

Fig. 3. Heat transfer coefficient at different heat fluxes (3000, 6000 and 9000 W/m^2) and constant mass flow rate $m = 125$ kg/m^2 s.

encountered. Some differences are also seen at low heat fluxes. As will be shown in successive sections, the range of experimental problems studied in this work are all dominated by the nucleate boiling phenomenon.

Where superheating of the vapour is considered, a well established correlation (such as the Gnielinski correlation) has been utilised for the calculation of the single-phase flow heat transfer coefficient.

4. Friction factor correlations

The prediction of pressure drops in direct-expansion evaporators is an important issue for the accurate design and optimisation of refrigeration, air-conditioning, and heat pump systems. The two-phase friction factor is estimated by using the Friedel correlation [29] because, under the working conditions of this study, it gives better results than others.

The total pressure drop, Δp_{total}, is the sum of the static pressure drop, Δp_{static}, the momentum pressure drop, Δp_{mom}, and the frictional pressure drop, Δp_{frict},

$$\Delta p_{\text{total}} = \Delta p_{\text{static}} + \Delta p_{\text{mom}} + \Delta p_{\text{frict}}. \tag{52}$$

The static pressure drop is set to zero as horizontal tubes are being considered, and the momentum pressure drop can be calculated directly by using the following equation:

$$\left(\frac{\mathrm{d}p}{\mathrm{d}z}\right)_{\text{mom}} = \frac{\mathrm{d}\left(\dot{m}_{\text{total}}/\rho_{\text{tp}}\right)}{\mathrm{d}z} \tag{53}$$

where ρ_{tp} is the homogeneous density of two-phase flow, $\dot{m}_{\text{total}}$ is the total mass flow rate through the pipe, and $(\mathrm{d}p/\mathrm{d}z)_{\text{mom}}$ is the momentum pressure gradient per unit length of the tube.

The frictional pressure drop is typically predicted by using a separated two-phase model and by applying a two-phase multiplier to the single-phase pressure drop (gas or liquid) in the tube.

4.1. Friedel correlation

This correlation uses the following multiplier:

$$\phi_{\text{LO}}^2 = E + \frac{3.24FH}{Fr_{\text{tp}}^{0.045}We^{0.035}} \tag{54}$$

where

$$E = (1-x)^2 + x^2\left[\frac{\rho_{\text{f}} f_{\text{GO}}}{\rho_{\text{G}} f_{\text{LO}}}\right], \tag{55}$$

$$F = x^{0.78}(1-x)^{0.224}, \tag{56}$$

$$H = \left(\frac{\rho_{\text{f}}}{\rho_{\text{G}}}\right)^{0.91}\left(\frac{\eta_{\text{f}}}{\eta_{\text{G}}}\right)^{0.19}\left(1-\frac{\eta_{\text{G}}}{\eta_{\text{f}}}\right)^{0.7}, \tag{57}$$

$$Fr = \frac{\dot{m}_{\text{total}}^2}{gD\rho_{\text{tp}}^2}, \tag{58}$$

$$We = \frac{\dot{m}_{\text{total}}^2 D}{\sigma \rho_{\text{tp}}}. \tag{59}$$

f_{GO} and f_{LO} are the gas and liquid friction factors, respectively, when flowing through the duct with the total mass velocity, $\dot{m}_{\text{total}}$. D stands for the equivalent diameter, σ is the surface tension, and ρ_{tp} the two-phase homogeneous density. The Friedel correlation is applicable to all vapour qualities ($0 \le x \le 1$), although Whalley recommends using it when

- Ratio of liquid and gas viscosities ($\eta_{\text{f}}/\eta_{\text{G}}$) < 1000.
- Total mass velocities $\dot{m}_{\text{total}}^2 < 2000\ \text{kg/m}^2\ \text{s}$.

For single-phase flow in pipes, the Petukhov correlation is considered in the case of turbulent flow, whereas the Blausius equation is used when laminar flow is encountered.

5. Air side heat transfer and friction factor correlations

In the description of the air processes, the correlations for heat transfer coefficients and friction factor, proposed by Chi-Chuan Wang et al. in [30], are used for dry air. These correlations update previous developments [31], and include a larger number of samples. The heat transfer coefficient is given in terms of the Colburn factor, $j = Nu/RePr^{1/3}$, so that it is given by:

$$j = \begin{cases} 0.108 Re_{D_c}^{-0.29} \left(\dfrac{P_t}{P_l}\right)^{P_1} \left(\dfrac{F_p}{D_c}\right)^{-1.084} \left(\dfrac{F_p}{D_h}\right)^{-0.786} \left(\dfrac{F_p}{P_t}\right)^{P_2} & \text{for } N = 1, \\ 0.086 Re_{D_c}^{P_3} N^{P_4} \left(\dfrac{F_p}{D_c}\right)^{P_5} \left(\dfrac{F_p}{D_h}\right)^{P_6} \left(\dfrac{F_p}{P_t}\right)^{-0.93} & \text{for } N \ge 2, \end{cases} \tag{60}$$

where,

$$P_1 = 1.9 - 0.23 \ln Re_{D_c}, \tag{61}$$

$$P_2 = -0.236 + 0.126 \ln Re_{D_c}, \tag{62}$$

$$P_3 = -0.361 - \frac{0.042N}{\ln Re_{D_c}} + 0.158 \ln\left(N \left(\frac{F_p}{D_c}\right)^{0.41}\right), \tag{63}$$

$$P_4 = -1.224 - \frac{0.076 \left(\dfrac{P_l}{D_h}\right)^{1.42}}{\ln Re_{D_c}}, \tag{64}$$

$$P_5 = -0.083 + \frac{0.058N}{\ln Re_{D_c}}, \tag{65}$$

$$P_6 = -5.735 + 1.21 \ln\left(\frac{Re_{D_c}}{N}\right). \tag{66}$$

The friction factor for dry air is given by:

$$f = 0.0267\, Re_{D_c}^{F_1} \left(\frac{P_t}{P_l}\right)^{F_2} \left(\frac{F_p}{D_c}\right)^{F_3} \tag{67}$$

where the coefficients are defined by:

$$F_1 = -0.764 + 0.739 \frac{P_t}{P_l} + 0.177 \frac{F_p}{D_c} - \frac{0.00758}{N}, \tag{68}$$

$$F_2 = -15.689 + \frac{64.021}{\ln Re_{D_c}}, \tag{69}$$

$$F_3 = 1.696 - \frac{15.695}{\ln Re_{D_c}}. \tag{70}$$

In the case of humid air, the proposed correlation for the Colburn factor is that derived in [14],

$$j = 19.36\, Re_{D_c}^{j_1} \left(\frac{F_p}{D_c}\right)^{1.352} \left(\frac{P_l}{P_t}\right)^{0.6795} N^{-1.291}, \tag{71}$$

where,

$$j_1 = 0.3745 - 1.554 \left(\frac{F_p}{D_c}\right)^{0.24} \left(\frac{P_l}{P_t}\right)^{0.12} N^{-0.19}. \tag{72}$$

In this case, the friction factor is given by:

$$f = 16.55\, Re_{D_c}^{f_1} \left(10\, Re_{\text{film}}\right)^{f_2} \left(\frac{A_o}{A_{p,o}}\right)^{f_3} \left(\frac{P_l}{P_t}\right)^{f_4} \left(\frac{F_p}{D_h}\right)^{-0.5827} \times \left(e^{D_h/D_c}\right)^{-1.117}, \tag{73}$$

where,

$$f_1 = -0.7339 + 7.187 \left(\frac{F_p}{P_l}\right)^{2.5} \left(\ln\left(9\, Re_{\text{film}}\right)\right), \tag{74}$$

$$f_2 = -0.5417 \ln\left(\frac{A_o}{A_{p,o}}\right) \left(\frac{F_p}{D_c}\right)^{0.9}, \tag{75}$$

$$f_3 = 0.02722\ \ln\left(6\, Re_{\text{film}}\right) \left(\frac{P_l}{P_t}\right)^{3.2} \ln Re_{D_c}, \tag{76}$$

$$f_4 = 0.2973 \ln\left(\frac{A_o}{A_{p,o}}\right) \ln\left(\frac{D_h}{D_c}\right). \tag{77}$$

Additional data and comments on these correlations may be found in the references mentioned above.

6. Experimental results

An experimental test campaign is carried out in order to study the performance of the fin and tube coil of a 20 kW air-to-water reversible heat pump for two different refrigerants, *R*-22 and *R*-290. In this section, the characteristics of the experimental installation, the measurements process,

and the conditions used to model the boiling process are described.

6.1. Experimental equipment

The test loop basically consists of three circuits: the air, water, and refrigeration loops. The instrumentation equipment installed permits the measurement of temperatures, mass flow rates, and pressures at all the relevant points of these loops. In what follows, the refrigerant loop is briefly described.

The experimental equipment used during the measurement campaign was a reversible heat pump, manufactured by CIATESA (model IWA-95). This heat pump was modified in order to obtain the optimum conditions during the testing process. The heat pump was equipped with: a hermetic four-cylinder reciprocating compressor; an inverter four ways valve; a thermostatic expansion valve; and two heat exchangers. One of these was a plate heat exchanger with 36 plates and a distributor, and the other was a fin and tube coil heat exchanger. Two coils were tested and their geometrical characteristics are gathered in Table 1.

The heat pump was constantly working in refrigeration mode, in such a way that the studied fin and tube heat exchangers were immersed in a closed space with controlled weather conditions of humidity and temperature. These weather conditions were determined by a sensor model HMP 143A, with an accuracy of $\pm 2\%$ for relative humidity and ± 0.1 °C for air temperature.

Fig. 4 shows a scheme of the experimental facility and the instrumentation used during the tests. The fin and tube heat exchangers were tested as evaporators of the heat pump, and the direction of the refrigerant was as displayed in the figure. The refrigerant inlet conditions in the evaporator were determined by the outlet conditions of the isenthalpic valve, so that the inlet vapour quality of the refrigerant at the heat exchanger was always greater than 0.

The relevant temperatures immediately before and after the heat exchanger and other at important devices of the heat pump were measured with calibrate PT-100 sensors, ± 0.1 K. Two viewing glasses were situated before and after the refrigerant store to determine any instability during the different performances.

Boiling pressure (P_{12}) and condensate pressure (P_1) were measured before and after the compressor with two Fisher Rosemount 3051 sensors, with an accuracy of ± 20 mbar. The same type of sensors were used to measure the pressure at the inlet and outlet of the heat exchangers, as Fig. 4 shows. In addition, the electric energy expended by the compressor was measured by means of a Schlumberger Quantum P200 energy counter, with an accuracy of $\pm 0.01\%$.

Table 1
Geometric parameters of measured Fin and tube coil heat exchanger

Heat exchanger model	RHPU	AHPU
External tube diameter (mm)	12.6	9.52
Internal tube diameter (mm)	11.9	8.92
Number of rows	3	4
Number of circuits	6	15
Number of tube per row	36	45
Tube material	Cu	Cu
Heat transfer area (refrigerant side) (m^2)	3.62	4.28
Circuit length (m)	16.15	10.2
Fin type	Wavy	Wavy
Fin material	Al	Al
Fin interval (mm)	2.1	2.5
Heat transfer area (air side) (m^2)	75.03	66.78

6.2. Measurements

Before the first measurements, the temperatures and mass flows in the experimental rig system have to be stabilised. The refrigerant level and possible appearance of bubbles in the flow of refrigerant were controlled through the viewing glasses for each measurement. The secondary fluid inlet temperatures on both the condenser and the evaporator were kept constant during the measurement process.

The superheating and subcooling temperatures of the refrigerant were determined with PT-100 sensors, situated at the inlet of the compressor and evaporator, respectively. All sensors were monitored by means of a data acquisition system and recorded in a computer during the measurement process every 10 s for each test. All the data files were processed on an in-house developed computer program named SIBC.

7. Modelling procedure

The governing equations described above are integrated in the ART© code environment [9]. The model is able to characterise the behaviour of each heat pump component allowing us to examine and analyse them separately.

As is commented above, experimental and calculated results obtained for the evaporation temperature have been compared when the fin and tube heat exchanger are used as evaporator. Different heat transfer correlations have been utilised in the evaporation temperature estimation in order to assess the behaviour of the model and study the influence of these correlation on the parameter calculations. Thus, it is not necessary to regard exactly the real working conditions and to specify the behaviour of all the heat pump components, but it is absolutely necessary to consider the same real working conditions for the heat exchangers studied. In this case, to describe properly the evaporator is enough to validate the solver and the correlations used by the model. The following considerations were taken into account in the computational description of the tests:

- For the correct evaporator definition, it is necessary to fix the inlet and the outlet. This is carried out by imposing superheating and taking into account that if

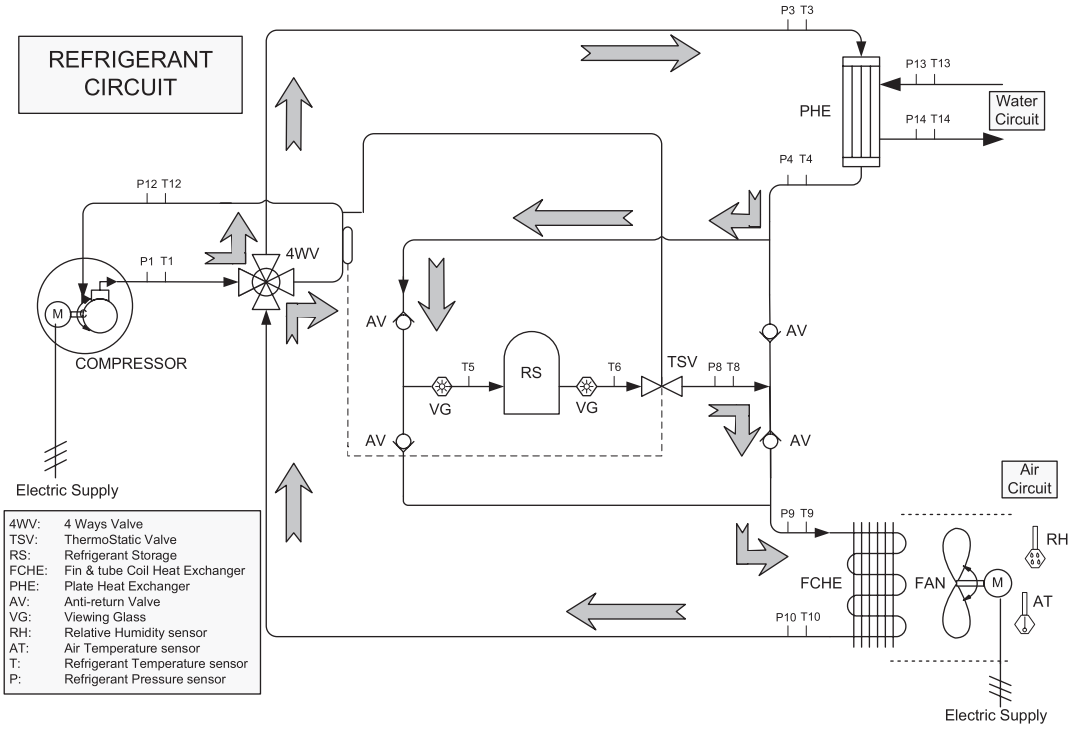

Fig. 4. Sketch of the experimental facility.

the expansion device is considered isenthalpic, the inlet is given when the outlet condensation temperature is known. These parameters are known from the experiments and are easy to fix in the code.

- Air inlet conditions (pressure, temperature, humidity, and mass flow rate of air) at the evaporator equal to the measured data obtained under weather controlled conditions during the tests, were imposed.
- In order to have the same outlet temperature at the condenser as in the experiment, an infinity-surface heat exchanger was considered. In this way, the outlet temperature is conditioned by the secondary fluid outlet temperature, which had been set equal to the condensation temperature measured in the experiments.
- Refrigerant mass flow rate has to be adjusted for any modelling point by tuning the cylinder capacity in

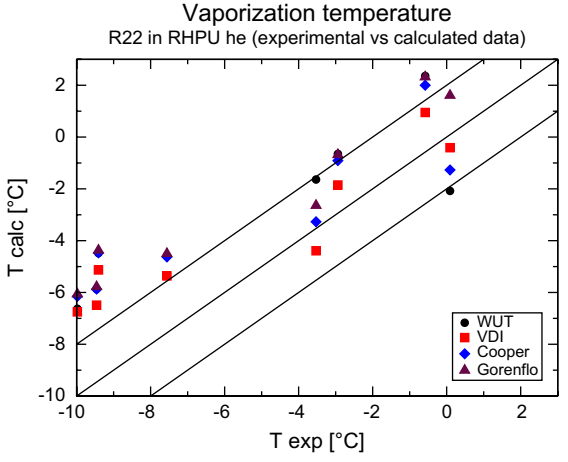

Fig. 5. Experimental results versus numerical results.

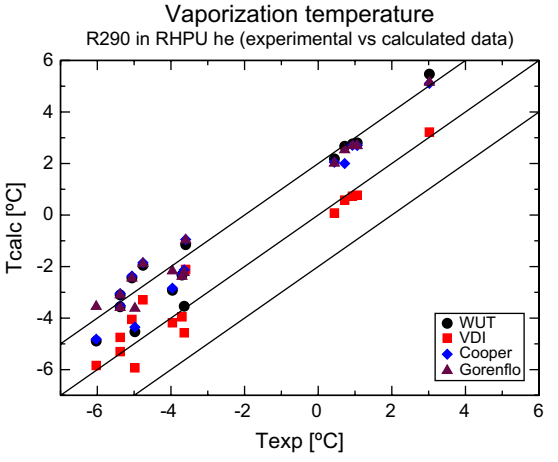

Fig. 6. Experimental results versus numerical results.

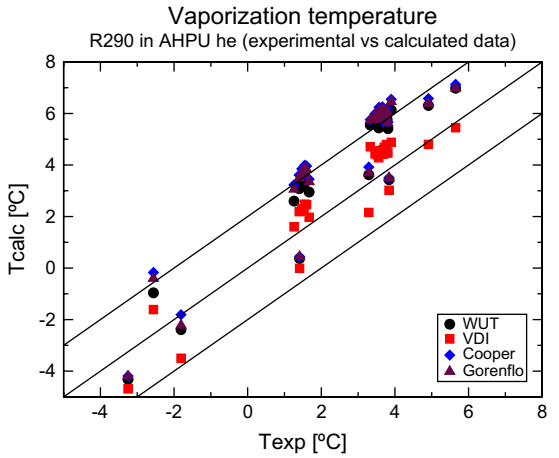

Fig. 7. Experimental results versus numerical results.

order to fit the same mass flow rate measured in the facility.

8. Experimental results versus calculated results

Several measurements were carried out, some of them using *R*-22 as the refrigerant and others using *R*-290. Furthermore, two kinds of fin and tube heat exchangers (RHPU and AHPU) have been studied.

Taking into account the boundary conditions imposed for the calculations (inlet conditions of air and refrigerant, and superheat at the evaporator outlet) the evaporation temperature is the correct value to compare, which is the ''free'' variable when an evaporator is inserted as a component in a system of this type with a thermostatic expansion device. Other authors choose the refrigeration capacity as a comparison variable. This quantity, however, is mainly determined by the mass flow rate provided by the compressor that is imposed as a boundary condition of the model, so surely our model can lie close to the experimental capacity regardless of the assumptions made or the correlations used. For this reason, the evaporation temperature is the correct value to compare. If the calculated value matches the experimental one, then we can be sure that the calculated capacity is the same as the experiment and also that the calculated COP of the unit is the same as the experiment.

The results obtained have been produced using the Wojtan et al. correlation, the VDI correlation, the Cooper correlation, and the Gorenflo correlation. The comparisons between the experimental results and the calculated values for the different correlations are displayed in Figs. 5–7. Lines corresponding to $\pm 2\,^{\circ}C$ differences have been depicted simply for the sake of comparison and clarity. These differences in evaporation temperature will produce differences between calculation and experiments of around 1% in cooling capacity and 2% in COP.

In most cases, the difference between experimental and computational results is lower than 2°. It should be remarked that the estimation of the evaporation temperature is not only influenced by the heat transfer correlation on the refrigerant side, but also by the uncertainties associated with the correlations used on the air-side (i.e. for the calculation of the heat transfer coefficient and the friction factor), and even by the uncertainties in the measurement processes. Similar tendencies and behaviours are shown for both refrigerants.

9. Conclusions

In this paper, a new philosophy in the analysis of refrigeration equipments is presented. Some aspects of the methodology employed in the numerical study and of the experimental facility used for its validation have been introduced. Several correlations corresponding to heat transfer coefficients on the refrigerant side and on the air side have been briefly described and afterward tested through the experimental and numerical results depicted here. Special attention has been paid to the boiling correlations inside horizontal tubes and some comparisons between them complete this work. In addition, some main conclusions can be highlighted:

- A model for fin and tube coils has been presented where the local variation of properties, friction factor, and heat transfer coefficient are adequately taken into account.
- The model has been tested with two different fin and tube heat exchanger geometries and for two different refrigerants.
- The global solution procedure and the iterative solution strategy (SEWTLE) used in the heat exchanger analysis have been proved to be effective enough to characterise the refrigeration cycle of a heat pump with the specifications mentioned in the paper.
- The use of the evaporation temperature as comparison parameter allows us to estimate the influence of the heat transfer coefficient in the cycle performance. This influence is, in fact, rather small in cycle parameters such as the COP or the cooling capacity. Supposing constant heat transfer coefficient, it has been proven that, changes in the heat transfer coefficient of about 50% of its original value lead to changes in the evaporation temperature greater than 100%. Its effect on other variables such as the COP are lower than 25% or even small in the case of the cooling capacity which varies about 5%.
- Four well established boiling correlations have been used in the model giving adequate accuracy when using in modelling evaporators working in real conditions. Also, it is remarkable that two of the correlations, Cooper and Gorenflo, are pool boiling correlations and work quite well, giving some

evidence that the nucleate part of the boiling heat transfer coefficient is dominant in the conditions tested.

Acknowledgements

This research has been partially financed by the following bodies: Fundación Séneca (CARM), project 00693/PPC/04 and Ministerio de Educación y Ciencia (MEC), project DPI2005-09262-C02-02.

The authors would like to acknowledge the experimental work carried out by Javier Blanco at the Universidad Politécnica de Valencia.

The authors also wish to thank Ms. Juana Mari Belchí and Ms. Neasa Conroy for assistance with the English translation.

References

[1] M. Browne, P.K. Bansal, An elemental ntu-e model for vapour-compression liquid chillers, International Journal of Refrigeration 24 (2001).

[2] L. Fu, G. Ding, Z. Su, G. Zhao, Steady-state simulation of screw liquid chillers, Applied Thermal Engineering 22 (2002).

[3] The DOE/ORNL Heat pump design model web page. <http://www.ornl.gov/sci/btc/hpdm.html>.

[4] The EVAP-CON Simulation model for finned-tube heat exchanger web page. <http://www2.bnfl.nist.gov/software/evapcond>.

[5] A. Bensafi, S. Borg, D. Parent, Cyrano: a computational model for the detailed design of plate-fin-and-tube heat exchangers using pure and mixed refrigerants, International Journal of Refrigeration 20 (1997).

[6] M.G. Cooper, Heat flow rates in saturated nucleate pool boiling, Advances in Heat Transfer 16 (1984) 157–239.

[7] D. Verein (Ed.), VDI Heat Atlas, VDI Verlag, 1993.

[8] L. Wojtan, T. Ursenbacher, J.R. Thome, Investigation of flow boiling in horizontal tubes: Part II. Development of a new heat transfer for stratified-wavy, dryout and mist flow regimes, International Journal of Heat and Mass Transfer 48 (2005) 2970–2985.

[9] J.M. Corberán, P. Fernández de Córdoba, J. Gonzálvez, F. Alias, Semiexplicit method for wall temperature linked equations (SEWTLE): a general finite-volume technique for the calculation of complex heat exchangers, Numerical Heat Transfer (2000) 37–59.

[10] G.B. Wallis, One-Dimensional Two-phase Flow, McGraw-Hill, Inc., 1969.

[11] J. Collier, J.R. Thome, Convective Boiling and Condensation, Oxford Science Publications, 1996.

[12] P.B. Whalley, Two-phase Flow and Heat Transfer, Oxford University Press, 1996.

[13] T.H. Kuehn, J.W. Ramsey, J.L. Threlkeld, Thermal Environmental Engineering, 3rd edition, Prentice Hall, Upper Saddle River, NJ, 1998.

[14] C.C. Wang, Y.T. Lin, C.J. Lee, An airside correlation for plain fin-and-tube heat exchangers in wet conditions, International Journal of Heat and Mass Transfer 43 (2000) 1869–1872.

[15] J.M. Corberán, M. García, Modelling of plate finned tube evaporators and condensers working with R134a, International Journal of Refrigeration 21 (4) (1998) 273–284.

[16] J.C. Chen, A correlation for boiling heat transfer to saturated fluids in convective flow, I&EC Process Design and Development 5 (1966) 322–329.

[17] M.M. Shah, Chart correlation for saturated boiling heat transfer: equations and further study, ASHRAE Transaction 88 (1982) 185–196.

[18] D. Steiner, J. Taborek, Flow boiling heat transfer in vertical tubes correlated by an asymptotic model, Heat Transfer Engineering 3 (1982) 43–69.

[19] S.S. Kutateladze, Boiling heat transfer, International Journal of Heat and Mass Transfer 4 (1961).

[20] K. Stephan, M. Abdelsalam, Heat transfer correlations for natural convection boiling, International Journal of Heat and Mass Transfer 23 (1980) 73–87.

[21] J.R. Thome, Engineering Data Book III, Wolverine, 2004.

[22] K. Stephan, P. Preusser, Wärmeübergang un maximale wärmestromdichte beim bechältersieden binäer und ternäer flüssingtsgemische, Chemie Ingenieur Technik 51 (1979).

[23] N. Kattan, J.R. Thome, D. Favrat, Flow boiling in horizontal tubes: Part 1. Development of a diabetic two-phase flow pattern map, Transaction of the ASME 120 (1998) 140–147.

[24] N. Kattan, J.R. Thome, D. Favrat, Flow boiling in horizontal tubes: Part 2. New heat transfer data for five refrigerants, Transaction of the ASME 120 (1998) 148–155.

[25] N. Kattan, J.R. Thome, D. Favrat, Flow boiling in horizontal tubes: Part 3. Development of a new heat transfer model based on flow pattern, Transaction of the ASME 120 (1998) 156–165.

[26] O. Zürcher, D. Favrat, J.R. Thome, Evaporation of refrigerants in a horizontal tube: an improved flow pattern dependent heat transfer model compared to ammonia data, Heat International Journal of Heat and Mass Transfer 45 (2002) 303–317.

[27] J.R. Thome, J. El Hajal, Two phase flow pattern map for evaporation in horizontal tubes, in: 1st International Conference on Heat Transfer, Fluid Mechanics and Thermodynamics, vol. 1, Kruger Park, South Africa; 8–10 April 2002, pp. 182–188.

[28] L. Wojtan, T. Ursenbacher, J.R. Thome, Investigation of flow boiling in horizontal tubes: Part I. A new diabetic two-phase flow pattern map, International Journal of Heat and Mass Transfer 48 (2005) 2955–2969.

[29] L. Friedel, Improved friction pressure drop correlations for horizontal and vertical two phase pipe flow, in: European Two Phase Flow Group Meeting, Paper E2, Ispra, Italy; 1979.

[30] C.C. Wang, Y.Y. Chi, Heat transfer and friction characteristics of plain fin-and-tube heat exchangers: Part II. Correlation, International Journal of Heat and Mass Transfer 43 (2000) 2693–2700.

[31] C.C. Wang, et al., Sensible heat and friction characteristics of plate fin-and-tube heat exchangers having plane fins, International Journal of Refrigeration 19 (1996) 223–230.